and journals most closely associated with the theme phrase within the database. In the example provided, where structures was the theme and the aircraft SCI database was examined, the nine most closely associated technology subcategories related to composites, airframes, materials design/analysis, fatigue/fatigue life, loads and dynamics, smart structures, NDI and system development. The most closely related authors were R. B. Heslehurst, S. N. Atluri, R. M. Measures, and F. W. Brust. Similarly, it was possible to determine the most closely related organizations (Georgia Institute of Technology, India Polytechnic Institute, University of Maryland, and the Federal Aviation Administration), journals (*Journal of Solids* and *Journal of Intelligent Material*) and countries (United States, England, Germany, and Australia) with what would appear to be a concentrated focus on structures because of their close proximity to the theme word structures within the aircraft SCI database.

Similarly, for the aircraft EC database, the most closely associated technology subcategories were the same as for the SCI database (just indicated), but now included a more significant presence in the loads and dynamics area. The most closely related authors were V. K and V. V. Varadan, C. C. Chamis, and R. B. Heslehurst. Organizations within the EC that were most closely tied to the structures theme were the Aeronautical Systems Center of Wright Laboratories and the American Helicopter Society, although many technical societies, such as the American Institute of Aeronautics and Astronautics, the American Society of Mechanical Engineers, the American Society of Civil Engineers, and the Society for Advancement of Material and Process Engineering publish extensively in the aircraft structures area. The *Journal of Solids* was the only journal that showed a close relationship to the structures theme. Although the United States and Australia both demonstrated a strong relationship to the theme of structures, it was Wales (University of Wales at Cardiff) that had the most direct relationship within the aircraft EC database.

III. Potential Areas of Additional Technology Effort

Based on the distribution of effort, represented by the published papers, over the past 7–8 years, it would appear that there are several areas that, in conjunction with recently expressed naval aviation priorities,[10] could benefit from increased attention and deserve a hard look for additional investment. These would include such areas as helo drive systems and gear boxes (longer life bearings); corrosion detection and prevention for both aircraft and support equipment; wireless sensors for aircraft health usage monitoring; advanced catapult designs; robotic systems for weapons and store handling; nuclear, biological and chemical protection systems; and training with increased use of simulation. All of the cited aircraft platform-related efforts have been listed by the naval aviation community as priority areas for increased capability, but, based on the published literature, have been receiving little in the way of technology support and effort.

IV. Conclusions

In summary, database tomography (DT) and bibliometrics would appear to be extremely effective tools for technology program managers in the development of an investment strategy. The process allows for the development of a very focused database that can be used for a variety of searches permitting the program manager to query the state of the art in a given technology (over the time span of database articles). In addition, through bibliometric analysis, the techniques allow for the determination of the most active and prolific researchers and organizations in the technical area. Highly cited authors, organizations, and journals can be determined. This will greatly assist the program manager as a new program plan is being developed by identifying and allowing for the possible interaction with the best talent in a given technology. Linchpin papers for a specific technology area can be identified as those most highly cited and will rapidly provide a current perspective on the state of the technology. One of the most powerful tools is the ability, through phrase frequency analysis, to summarize, categorize, and quantify large amounts of textural technical information so that a global picture or perspective emerges. Last, through the use of DT, closely related themes to a given technology can be identified and pursued.

References

[1] Kostoff, R. N., Green, K. A., Toothman, D. R., and Humenik, J. A., "Database Tomography Applied to an Aircraft Science and Technology Investment Strategy," TR NAWCAD PAX/RTR-2000/84, Naval Air Warfare Center Aircraft Division, Patuxent River, MA, 2000.

[2] Science Citation Index, Inst. for Scientific Information, 3501 Market Street, Phila, PA 19104.

[3] E I Compendex, Engineering Information Inc., Hoboken, NJ.

[4] Kostoff, R. N., Eberhart, H. J., and Miles, D. L., "System and Method for Database Tomography," U.S. Patent 5440481, 1995.

[5] Kostoff, R. N., Eberhart, H. J., and Toothman, D. R., "Database Tomography for Information Retrieval," *Journal of Information Science*, Vol. 23, No. 4, 1997, pp. 301–312.

[6] Kostoff, R. N., Eberhart, H. J., and Toothman, D. R., "Database Tomography for Technical Intelligence: A Roadmap of the Near-Earth Space Science and Technology Literature," *Information Processing and Management*, Vol. 34, No. 1, 1998, pp. 69–85.

[7] Kostoff, R. N., Eberhart, H. J., and Toothman, D. R., "Hypersonic and Supersonic Flow Roadmaps Using Bibliometrics and Database Tomography," *Journal of the American Society for Information Science*, 15 April 1999, pp. 427–447.

[8] Kostoff, R. N., Braun, T., Schubert, A., Toothman, D. R., and Humenik, J. A., "Fullerene Roadmaps Using Bibliometrics and Database Tomography," *Journal of Chemical Information and Computer Science*, Vol. 40, Jan.–Feb. 2000, pp. 19–39.

[9] Bradford, S. C., "Sources of Information on Specific Subjects," *Engineering*, 1934, p. 137.

[10] Nathman, J. B., "Science and Technology Prioritized Capabilities-Information Memorandum," Memorandum 16 Nov. 1998, Air Warfare Div., Chief of Naval Operations, 1998.

Fast and Robust Viscous/Inviscid Interaction Code for Wing Flowfield Calculations

Urpo J. Pesonen,* Ramesh K. Agarwal,† and Seppo Laine‡
Wichita State University, Wichita, Kansas 67260

Introduction

IN this study[1] a three-dimensional potential solution has been combined with two-dimensional viscous/inviscid interaction flow analysis at several cross sections across the wing span. With the assumption of no crossflow at these stations, the method provides a flow solution with the viscous effects taken into account. The two-dimensional flow solver used in the new combined method is XFOIL,[2] which has a built-in two-dimensional panel code, and a viscous/inviscid interaction solver, which is based on empirical formulas. One remarkable property of this flow solver is that it treats the boundary-layer edge velocity as the sum of the inviscid part and the viscous part, which embodies the effect of viscous/inviscid interaction. Therefore, the inviscid solution can come from anywhere and is totally independent of the viscous solution. In the combined method the two-dimensional panel code in XFOIL is bypassed, and instead, a cross section of the three-dimensional panel solution is read in and treated as a two-dimensional solution.

Received 10 May 1999; presented as Paper 99-3139 at the 17th Applied Aerodynamics Conference, Norfolk, VA, 28 June–1 July 1999; revision received 1 March 2000; accepted for publication 1 March 2000.

*Graduate Research Assistant, Department of Aerospace Engineering. Student Member AIAA.

†Bloomfield Distinguished Professor and Executive Director, National Institute for Aviation Research. Fellow AIAA.

‡Professor of Aeronautical Engineering; currently Professor, Helsinki University of Technology, Espoo, Finland. Associate Fellow AIAA.

The three-dimensional panel code used to provide the inviscid velocities at cross sections is HISSS by L. Fornasier.[3] It uses a linear source distribution and quadratically varying doublet strengths to represent the thickness of the configuration and the generated lift. Once the inviscid three-dimensional solution is computed for a specific angle of attack, XFOIL is used at numerous stations across the wing span and force, and moment coefficients for the whole wing are integrated from these results.

Because of XFOIL's capability to predict transition, separation, and laminar separation bubbles, the new method is especially applicable to low-Reynolds-number flows and even high angles of attack. These are challenging areas for any flow solver, and a reliable code could be of great value for general aircraft, sailplane, and hydrofoil design. On traditional fuselages the boundary-layer effects cannot be computed because of considerable crossflow velocities. However, in such a case the whole configuration could first be computed with the panel method, and then the viscous/inviscid interaction solver could be applied to the wings.

Objectives in designing this sort of an analysis tool are accuracy, ease of use, good convergence, applicability to a wide range of configurations and flows, and computational efficiency. Even when a Navier–Stokes (N–S) or Euler solver might give more accurate results, the effort of generating the necessary volume grid and the extensive computational time required might outweigh the improved accuracy.

The new method was constructed by modifying HISSS and XFOIL so that they can be used in combination. A rectangular wing with a NACA 0012-airfoil and a highly swept wing with taper, twist, and a cambered airfoil were analyzed, and the results were compared to experimental data and a N–S solution.

Validation of the Method

Test Case I : Rectangular Wing

Pressure distributions at spanwise cross sections and the C_N vs α curve for a rectangular wing with a NACA 0012 airfoil was computed, and the results were compared to experimental data presented by Yip and Shubert[4] and a N–S solution computed with the FINFLO parallel multiblock flow solver.[5]

A rectangular wing with a NACA 0012 airfoil, aspect ratio $A = 5.90$, chord $c = 1.0$ m, and no sweep was computed with a Reynolds number of 3.37×10^6 and a Mach number of 0.14. Pressure distributions have been measured at 10 cross sections along the wing span by Yip and Shubert[4]. The panel model of this wing is shown in Fig. 1.

FINFLO is a parallel multiblock flow solver designed in the Laboratory of Aerodynamics at Helsinki University of Technology. The code is described in Ref. 5. For this test case a three-dimensional volume grid of size $198 \times 80 \times 80 = 1{,}267{,}200$ was created to model half of the wing. The turbulence model used was k–ω supersonic transport, and the transition on both surfaces was fixed at $x/c = 0.05$ as with the combined method.

Three different angles of attack were computed: $\alpha = 6.75$, 15.16, and 19.35 deg. The first two cases clearly converged, but the N–S solution for the highest α ended up oscillating within $\Delta C_N \approx 0.1$ of $C_N = 0.86$; obviously, this solution predicted massive flow separation on the wing. This can also be seen in Fig. 1.

The pressure coefficients were compared to experimental results,[4] and such a comparison for $\alpha = 6.75$ deg is shown for a middle cross section in Fig. 1. The results agree remarkably well with the experiment—except for the wing tip area, where the assumption

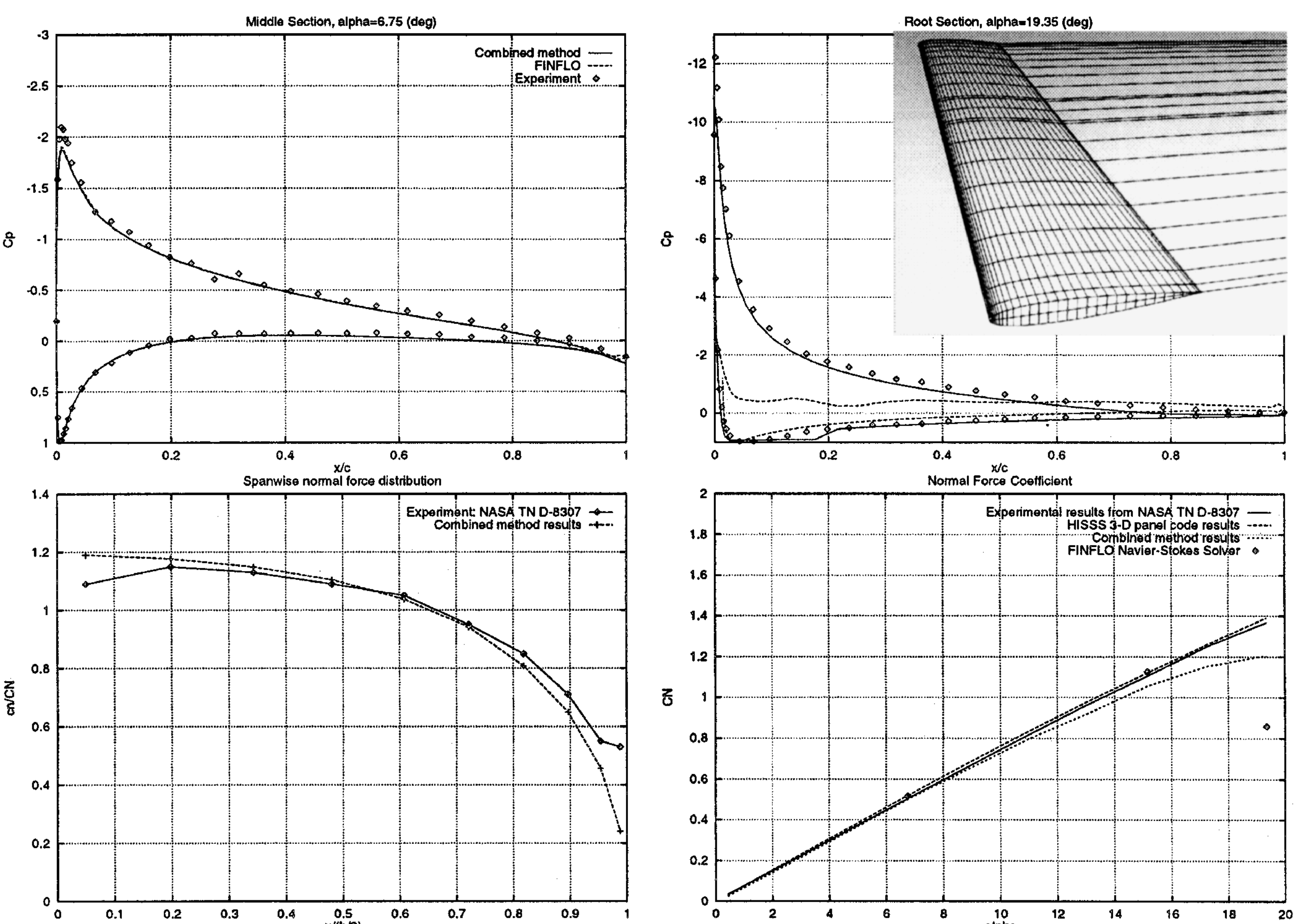

Fig. 1 Rectangular wing with a NACA 0012 airfoil, $A = 5.90$. Results compared to experimental data and a N–S solution. C_p distributions for $\alpha = 6.75$ and 19.35, spanwise lift distribution for $\alpha = 6.75$, and normal force vs α. $Ma = 0.14$ and $Re = 3.37 \times 10^6$.

of two-dimensional flow is not valid anymore. Everywhere along the span there appears to be a slight underestimation of the suction peak close to the leading edge. In an attempt to predict the peak pressures more accurately, higher panel densities in this area were tried, but they had no notable effect on the results. On the other hand, the agreement of the combined method solution with the FINFLO solution is remarkable. This gives a reason to suspect that the wind-tunnel corrections in Ref. 4 might have been insufficient.

Another source for error in the measurements might be the finite round plate that the semispan wing was mounted on. It does not act like a larger wall in the sense that there is a drop in the normal force distribution at the root of the wing (see Fig. 1). This represents a smaller effective aspect ratio, and thus, especially at high angles of attack, the lift curve slope becomes less steep and the stall postponed to a higher angle of attack. In Fig. 1 there is also a similar comparison at the wing root section at an angle of attack of $\alpha = 19.35$ deg. At such a high angle of attack the combined method seems to be more reliable than the N–S solution, but it is possible that in reality a whole wing of aspect ratio $A = 5.9$ might actually stall much earlier than the half-span model used in the experiments.

Eventually, the C_N vs α curve was plotted (Fig. 1) for the three-dimensional panel code results, the experimental data of Ref. 4, the combined method results, and the FINFLO N–S solution. The result is very surprising: For $\alpha = 4$ deg $\cdots$ 10 deg the combined method and the FINFLO solution are both closer to measurements than the panel method solution, but for greater angles of attack first the combined method solution deviates from the experimental data predicting stall, and later the FINFLO solution shows a radical loss of lift. Toward $\alpha = 19.35$ deg the panel method solution gives the best accuracy! This is very unexpected because the panel code does not take viscosity into account at all. It seems like this test case is very sensitive to a possible difference in the effective aspect ratio and the Reynolds number.

In overall accuracy the error of the new method solution ranges from $\Delta C_N \approx 0.004$ at $\alpha = 6.75$ deg to $\Delta C_N \approx 0.16$ at $\alpha = 19.35$ deg—the first result being remarkably good. The FINFLO-result, on the other hand, is more accurate at $\alpha = 15.16$ deg. A significant result for the new method is the short time required for computation. The panel code took about 30 min for the initial inviscid three-dimensional solution with 875 panels on an R5000 processor, but for each new angle of attack it only took a couple of minutes. XFOIL solves each two-dimensional case in several seconds, but especially at high angles of attack it is necessary to start first with smaller α and Reynolds numbers to achieve convergence. The ease of creating only surface paneling as opposed to a three-dimensional volume grid required by Euler and N–S solvers is a benefit of the new method.

Test Case II: Swept Wing

As the second test case, a wing with considerable sweep was chosen to evaluate the new method's sensitivity to crossflow at the wing stations, where the boundary-layer analysis was done. At each wing station the flow is assumed to be two-dimensional, and any crossflow from the inviscid panel solution is disregarded. When the spanwise flow component becomes significant, this assumption can lead to severe errors in the final solution. To find out how sensitive the method is, a highly swept wing was analyzed at different angles of attack, and the results were compared with experimental data provided in Ref. 6.

The wing had 45 deg of sweepback, an aspect ratio of 3, a taper ratio of 0.5, and 5 deg of washout between the root and the tip. The airfoil sections perpendicular to the quarter-chord line were the

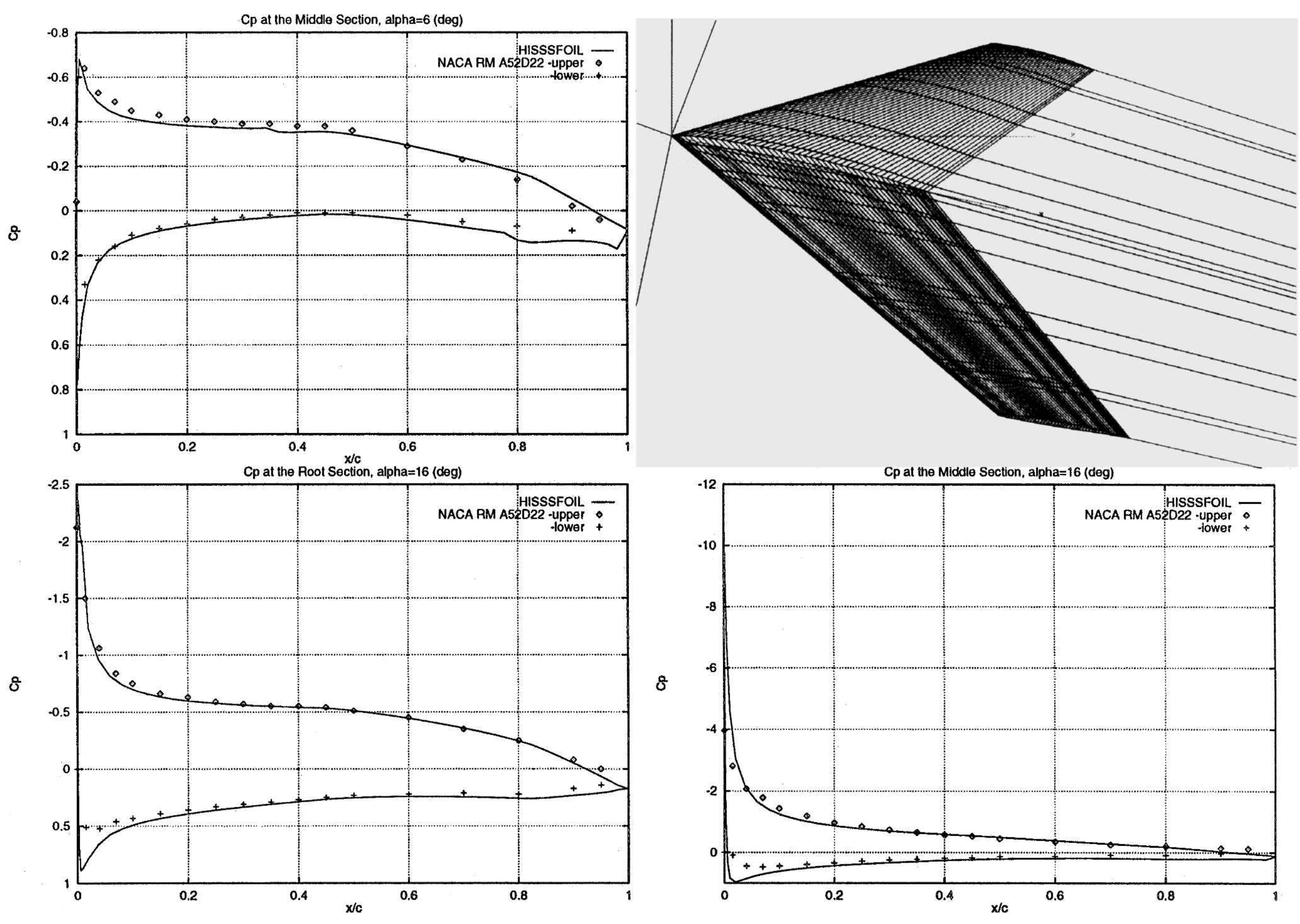

Fig. 2 Swept wing with a NACA 64A410 airfoil, $A = 3.0$, $\Lambda_{1/4} = 45$ deg. Computed C_p distributions compared to experimental data for $\alpha = 6$ deg at $y/(b/2) = 0.71$ and for $\alpha = 16$ deg at $y/(b/2) = 0.09$ and $y/(b/2) = 0.71$. $Ma = 0.25$ and $Re = 4 \times 10^6$.

NACA 64A410. The Reynolds number was 4×10^6, and the Mach number was 0.25. The computed pressure coefficients were compared to experimental results,[6] and such a comparison for $\alpha = 6$ deg is shown for a middle cross section in Fig. 2. The combined method solution agreed quite well with the experiment at the root and middle sections of the wing, but there was a notable underestimation of the top surface suction at the tip station. At the tip also the computed results near the trailing edge seem unnatural and different from the experiment. It is likely that this is caused by wing tip vortices and increased spanwise flow that the new method cannot handle. Similar comparisons at a higher angle of attack, $\alpha = 16$ deg, are shown in Fig. 2 for the root and middle sections. Even for such high sweep the solution at wing root (where the assumption of two-dimensional flow is valid) seems remarkably accurate at such a high angle of attack. Yet, at the stations closer to the tip there were some convergence problems with the boundary-layer computation, and it can be seen that the method dramatically overshoots the minimum C_p value. Yet, the results show that for moderate angles of attack even a highly swept wing can be analyzed with this method with good reliability.

Conclusions

The combined three-dimensional viscous/inviscid analysis method introduced in this Note gave reasonably accurate results with a short computational time in the calculated test cases. The method is especially suitable for low-Reynolds-number flows because of its capability of predicting transition and representing laminar separation bubbles. As a tool for analyzing wings, the code is several orders faster than a N–S solver, and creating the surface paneling is much easier a task than generating a three-dimensional volume grid.

However, the method assumes two-dimensional flow at the cross sections where the boundary-layer is computed, which is not realistic at the wing tip, especially on highly swept wings at high angles of attack. Neglecting possible crossflow instabilities can also cause errors in the transition prediction for swept wings. Therefore, the method is limited to only moderate sweep angles, or only low angles of attack for high sweep and is not suitable for small aspect ratio wings. The panel method HISSS breaks down in transonic flow, and XFOIL, on the other hand, only works for subsonic flows. These facts limit the applicable range of the combined method to subsonic flows.

This method can readily be used for analysis of more complex configurations as long as the assumption of two-dimensional flow is not violated on the surfaces analyzed. On bulging bodies or vertical surfaces, only an inviscid solution can be computed, and viscosity will not be taken into account. However, this sort of analysis might still give acceptable results at least for lift because the error in the contribution of a fuselage will not be significant in the integrated results. Analysis of sailplanes or general aviation aircraft are self-evident applications, but the method could also be used for analysis of blended wing body designs and hydrofoils.

References

[1]Pesonen, U., Agarwal, R., and Laine, S., "A Fast and Robust Viscous/Inviscid Interaction Code for Wing Flowfield Calculations," AIAA Paper 99-3139, June 1999.

[2]Drela, M., "XFOIL: An Analysis and Design System for Low Reynolds Number Airfoils," *Low Reynolds Number Aerodynamics*, Springer–Verlag, New York, 1989.

[3]Fornasier, L., "HISSS—A Higher-Order Panel Method for Subsonic and Supersonic Attached Flow About Arbitrary Configurations," Messerschmitt, Rept. LKE122-S-PUB-319, Bölkow, Blohm GmbH, 1987.

[4]Yip, L., and Shubert, G., "Pressure Distributions on a 1- by 3-meter Semispan Wing at Sweep Angles from 0° to 40° in Subsonic Flow," NASA TN D-8307, Dec. 1976.

[5]Kaurinkoski, P., and Hellsten, A., "FINFLO: the Parallel Multi-Block Flow Solver," Helsinki Univ. of Technology, Espoo, Finland, Lab. of Aerodynamics, Rept. A-17, Jan. 1988.

[6]Boltz, F., and Kolbe, C., "The Forces and Pressure Distribution at Subsonic Speeds on a Cambered and Twisted Wing Having 45° of Sweepback, and Aspect Ratio of 3, and a Taper Ratio of 0.5," NASA RM-A52D22, July 1952.

Proposed Mechanism for Time Lag of Vortex Breakdown Location in Unsteady Flows

Ismet Gursul*
University of Bath, Bath, BA2 7AY, United Kingdom

Introduction

EXPERIMENTS show that a time lag of breakdown location is observed in all unsteady flows regardless of the source of the unsteadiness. The dynamic response of breakdown location is similar to that of a first-order system. It is suggested in this Note that the time constant is essentially the same for all of the excitations and that the mechanism of the time lag with respect to the quasi-steady case is universal. This universality may originate from the wave propagation properties of the vortex flows. A simple model of time lag of vortex breakdown location was proposed, and the predictions were compared with the experiments.

The time lag of vortex breakdown location with respect to its variation in the quasi-steady case has been observed for several types of wing motion including pitching, plunging, and rolling. Recently, more detailed observations of the phase lag were made by Atta and Rockwell,[1] LeMay et al.,[2] and others. These studies revealed that, for a periodic pitching motion, vortex breakdown location forms hysteresis loops when plotted as a function of angle of attack because of the time lag of breakdown location. It was also shown that the phase lag increases with increasing reduced frequency, without significant influence of Reynolds number. The response of breakdown location was also studied for transient motions such as a finite ramp pitching motion or plunging motion by Thompson et al.,[3] Reynolds and Abtahi,[4] and others. Similar observations of time lag and hysteresis effects were made for pitch-up and pitch-down motions. It has been found that the response of breakdown location is similar to that of a first-order system. The time constant τ can be estimated from the time history of breakdown location in response to a given unsteady wing/surface motion. The estimated values of the time constant for different types of motion are given by Srinivas et al.[5] and Greenwell and Wood.[6] Although the normalized time constant $\tau U_\infty / c$ is affected by the type and amplitude of the motion, the breakdown location in the static case, and the sweep angle of the wing, it value falls between $\tau U_\infty / c = 1$–2 for slender wings ($\Lambda \geq 70$ deg). By curve fitting to the experimental values of the phase lag for pitching wings, Greenwell and Wood[6] obtained $\tau U_\infty / c = 1.67$. In summary, the time constant can be considered essentially the same for different wing/surface motions as a first approximation.

Recent investigations of vortex breakdown control techniques revealed similar time lags. The measured phase lag of breakdown location with respect to the quasi-steady case is shown in Fig. 1 as a function of the reduced frequency $K = \omega c / 2U_\infty$ for the oscillating leading-edge flaps[7] and leading-edge extensions[8] together with the pitching wings.[2,9] Although there is a larger scatter of data at high frequencies, there is a consistent trend of increasing phase lag with increasing reduced frequency. Several factors may contribute to the data scatter: the breakdown location in the static case; the amplitude of the motion; fluctuations of breakdown location, which are also observed for stationary wings; the number of cycles used for phase averaging; and the method used to calculate the phase lag. With these factors in mind, we do not expect a collapse of data for different motions. The purpose of Fig. 1 is simply to show that the phase lags are similar for α, Λ, and δ variations.

Received 22 May 1999; revision received 17 April 2000; accepted for publication 18 April 2000.

*Reader in Aerospace Engineering, Department of Mechanical Engineering.